

# Communication

## Influence of Solid-State Diffusion during Equilibration on Microstructure and Fatigue Life of Superalloy Wide-Gap Brazements

L.O. OSOBA and O.A. OJO

The influence of solid-state diffusion-controlled solute-loss into additive powder particles (APPs), as determined by particles size, during the equilibration stage of wide-gap brazing, on microstructure and fatigue behavior of a brazed aerospace superalloy was studied. The results, which experimentally confirm previously reported numerical model simulation results, show that, in order to avoid degradation of fatigue life of wide-gap brazement, adequate solute-loss into the APPs, which is necessary to prevent their complete melting, but has not been generally considered, is imperative.

DOI: 10.1007/s11661-013-1849-x

© The Minerals, Metals & Materials Society and ASM International 2013

Precipitation-strengthened cast nickel-based superalloys are used for manufacturing hot-section components of aero and land-based gas turbine engines, because of their remarkable high temperature mechanical strengths and hot-corrosion resistance. The demand for higher efficiencies, which require turbine engines to operate at higher temperatures, has led to increased degradation of engine components through higher levels of creep, fatigue, and oxidation. It is generally more economically attractive to repair damaged parts instead of going for a complete replacement. Traditional repair techniques, such as welding, are commonly used in the repair of many superalloy components. However, precipitation-strengthened cast nickel-based superalloys, like Inconel 738 (IN 738), are generally difficult to weld because of their high susceptibility to weld cracking.<sup>[1-6]</sup> Wide-gap brazing is an alternate technique for joining and repairing gas turbine engine components made of difficult-to-weld superalloys.<sup>[7-11]</sup> The technique often involves the use of composite powder mixture as the interlayer material. The powder mixture consists of regular brazing filler alloy powder that contains melting point-depressant (MPD) solute and an additive powder

alloy that is essentially free of the MPD solute, usually the base-alloy powder. The use of the powder mixture reduces undesirable liquid-phase erosion of the base material and also enables desirable enrichment of the joint region with the base-material alloying element for enhanced joint properties.

During wide-gap brazing, the brazing powder particles (BPPs), which normally have a lower melting temperature than that of the additive powder particles (APPs), melt completely, which in turn produces solutal melting of the APPs. It is generally assumed that APPs only undergo partial melting during wide-gap brazing. The main thrust for the solutal melting of the APPs into the surrounding molten brazing filler alloy is to reduce the concentration of the MPD solute in the liquid to the equilibrium liquidus value at the brazing temperature. In analytic brazing models, this equilibration process is often assumed to exclusively involve the addition of solvent element from the solid powder particles to the surrounding liquid without concomitant transfer of the MPD solute from the liquid into the particles by solid-state diffusion within the particles.<sup>[12]</sup> This is due to the difficulty in modeling simultaneous solid-state solute-transport within APPs and their melting by the surrounding liquid. Nevertheless, a recent more rigorous and robust numerical modeling of the process has shown that equilibration of the liquid occurs not only by solutal melting of the APPs but also through solid-state diffusion-controlled solute-loss from the liquid into the APPs.<sup>[13]</sup> The analysis shows that for a given volume ratio of APPs to BPPs, the extent of solutal melting of the APPs is influenced by the extent of the solute-loss into the APPs. A factor that significantly influences the extent of solute-loss is the size of the APPs. Accordingly, the main objective of the current research, is to study the extent of solute-loss effect, as determined by the size of APPs, on the microstructure and fatigue life of a wide-gap brazement of IN 738 superalloy, and the results of the study are reported and discussed in this communication.

The base-alloy used in this study is cast polycrystalline IN 738 superalloy with the chemical composition of (wt pct) 0.11C, 15.84Cr, 8.5Co, 2.48W, 1.88Mo, 0.92Nb, 0.07Fe, 3.46Al, 3.47Ti, 1.69Ta, 0.04Zr, 0.012B, and balance nickel. The brazing filler alloy that was used was Nicrobraz 150 with the chemical composition of (wt pct) 15Cr, 3.5B, 0.03C, and balance Ni. Two types of IN 738 superalloys powder with different particle sizes, fine and coarse, of averages sizes of 25 and 85  $\mu\text{m}$ , respectively, were used as the APPs. A mixture of 50 pct BPPs and 50 pct APPs was used to produce two types of interlayer materials, one containing the fine APPs and the other containing the coarse APPs. In addition, for baseline comparison, a 100 pct brazing alloy powder was also used for brazing some specimens. The wide-gap brazing, in the form of surface deposition to simulate surface damage repair (Figure 1), was performed in a brazing vacuum furnace at a pressure of  $\sim 10^{-5}$  Torr, at 1423 K (1150 °C) for 1 hour. Brazed specimens were sectioned by the EDM and prepared by standard metallographic techniques for microstructural examination by optical microscopy (OP) and scanning electron microscopy (SEM) techniques. Initial OP

L.O. OSOBA, Lecturer, formerly with Department of Mechanical and Manufacturing Engineering, University of Manitoba, Winnipeg, MB R3T 5V6, Canada, is now with Department of Metallurgical and Materials Engineering, University of Lagos, Lagos, Lagos State, Nigeria. O.A. OJO, Professor, is with the Department of Mechanical and Manufacturing Engineering, University of Manitoba. Contact e-mail: olanrewaju.ojo@ad.umanitoba.ca

Manuscript submitted November 25, 2012.

Article published online July 9, 2013

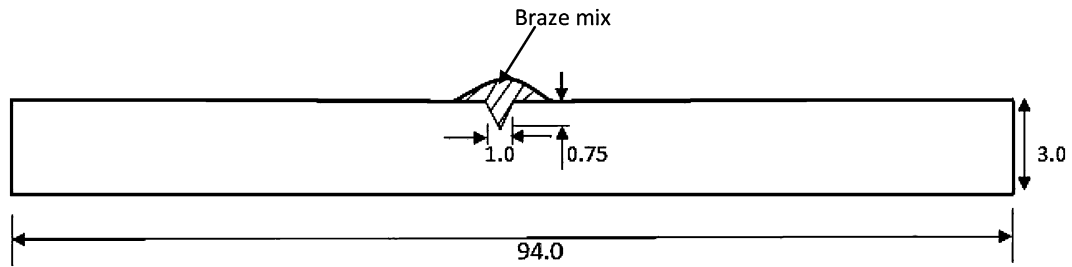


Fig. 1—Schematic of the surface deposition wide-gap brazement specimen (all dimensions in mm).

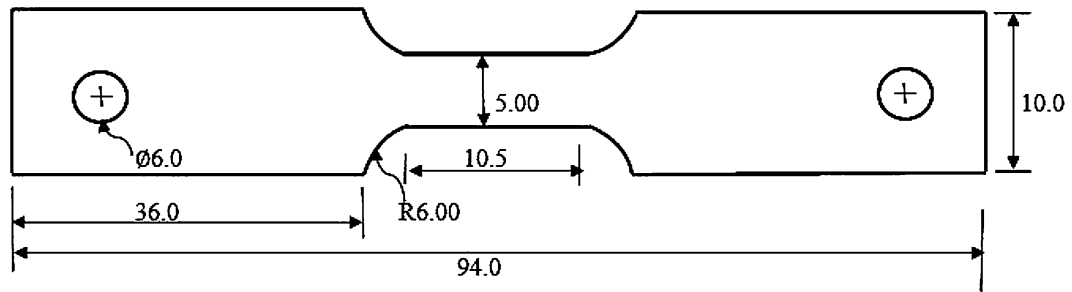


Fig. 2—Fatigue testing specimen (all dimensions in mm).

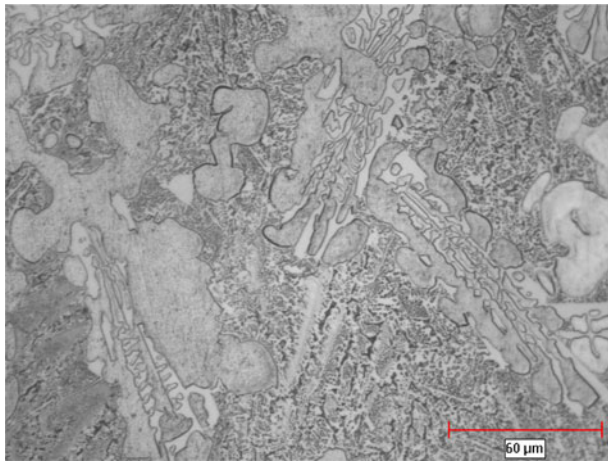


Fig. 3—Microstructure a brazement produced with fine APPs.

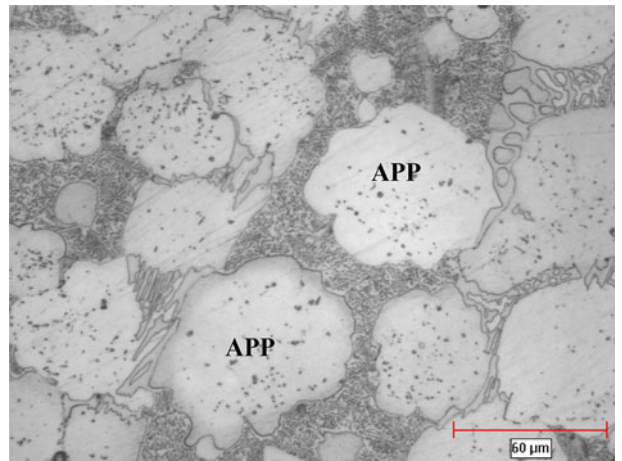


Fig. 4—Microstructure of a brazement produced with coarse APPs.

assessment of the joint microstructure was performed by means of an inverted-reflected light microscope equipped with a CLEMEX Vision 3.0 image analyzer. Further microstructural study (using secondary and backscattered electron imaging modes) and chemical compositional analysis of the brazements were performed on a JEOL 5900 SEM, equipped with an ultrathin window Oxford energy dispersive spectrometer (EDS) system equipped with an INCA software. The microhardness values of different regions in the brazed joint were measured by means of Buehler microhardness tester with a load of 300 g. Fatigue testing of brazed specimens, with dimensions shown in Figure 2, was

performed by means of a Instron servo-hydraulic fatigue testing machine at a stress of 284 MPa and a frequency of 2 Hz.

A typical microstructure of the brazement produced using the powder mixture that contained the fine APPs is presented in Figure 3. The entire microstructure consists of eutectic-type microconstituents with no evidence of residual APPs. In contrast, however, the microstructure of the brazement produced with coarse APPs, as shown in Figure 4, consists of a mixture of remnant of partially melted APPs and eutectic-type microconstituents that are similar to the eutectic observed in the brazement of the fine APPs. SEM-EDS

**Table I. SEM-EDS Semi-Quantitative Metallic Composition of Eutectic Microconstituents in the Brazements**

Elements	Cr-Rich Phase (Atomic Percent)	Ni-Rich Phase (Atomic Percent)	Solid Solution Phase (Atomic Percent)
Al	—	2.90	6.32
Ti	0.29	4.29	1.71
Cr	84.70	9.35	15.76
Co	1.99	4.97	4.53
Ni	6.02	78.42	71.03
W	3.03	0.09	0.58
Mo	4.15	—	—

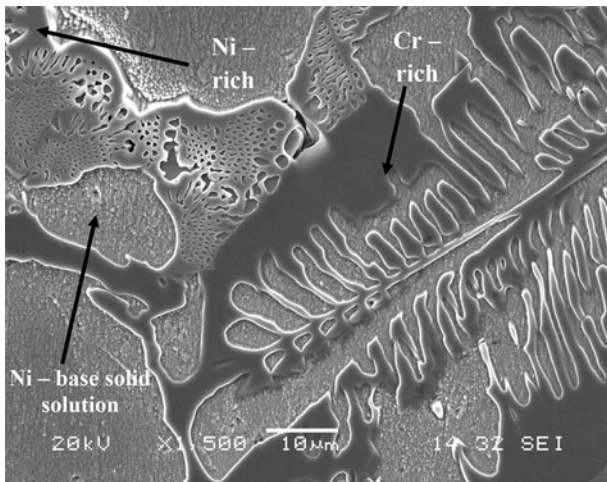


Fig. 5—SEM micrograph showing the eutectic microconstituents in the brazement.

metallic semi-quantitative compositional analysis (Table I; Figure 5) shows that the eutectic-type products in both brazements consist of nickel-rich and chromium-rich boride phases, and nickel-based solid-solution phase. It is known that during wide-gap brazing, the BPPs melt when the temperature reaches the melting temperature of the alloy, which in the case of this study is 1323 K (1050 °C). Equilibration process after melting of the BPPs produces solutal melting of the APPs by the surrounding molten brazing alloy. Nonequilibrium solidification reaction products are produced from the liquid during subsequent cooling from brazing temperature. Ohsasa *et al.*<sup>[14]</sup> in their numerical modeling of diffusion brazing of Ni, used Scheil simulation to calculate the on-cooling solidification behavior of the residual liquid produced by Ni-Cr-B filler alloy. They reported that the liquid solidifies by eutectic reactions to produce eutectic products consisting of nickel-rich and chromium-rich boride phases, and nickel-rich solid solution. Also, a schematic of the liquidus projection of the nickel-rich corner of Ni-Cr-B ternary phase diagram, according to Villars *et al.*<sup>[15]</sup>, is shown in Figure 6. According to the diagram, nickel-rich and chromium-rich borides are possible products of monovariant eutectic-type reaction. The lowest solidification temperature in the system is at point E<sub>2</sub> on the diagram,

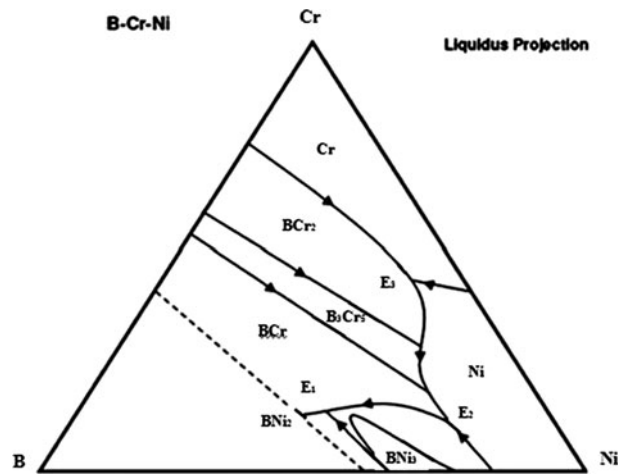


Fig. 6—Schematic projection of nickel-rich corner of Ni-Cr-B ternary system in Ref. [14].

where solidification terminates by an invariant ternary eutectic-reaction producing nickel-rich and chromium-rich boride phases and nickel-rich solid solution. The terminal solidification temperature is below the bonding temperature used in the current study. Therefore, the observation that the entire microstructure of the fine APPs brazement consists of the eutectic products, while only part of the microstructure of the coarse APPs brazement contains the eutectic products, confirms that complete and partial meltings of the fine and coarse APPs occurred, respectively, during brazing. This is further evident by the fact that the microstructure of the fine APPs brazement looks similar to that of a brazement produced by using 100 pct BPPs, which completely melts at 1050 °C (1323 K) (Figure 7). The fact that complete and partial meltings occurred in the fine and coarse APPs brazements, respectively, even though both contained 50 pct APPs, can be explained by the effect of solid-state diffusion-controlled solute-loss from the liquid into the APPs. It has been found that, in our previous study through numerical modeling,<sup>[13]</sup> the extent of solutal melting of APPs is directly influenced by the kinetics of solute transport within the APPs during equilibration process. At a given volume ratio of APPs to BPPs, the higher the rate and extent of solid-state diffusion-controlled solute-transport within the



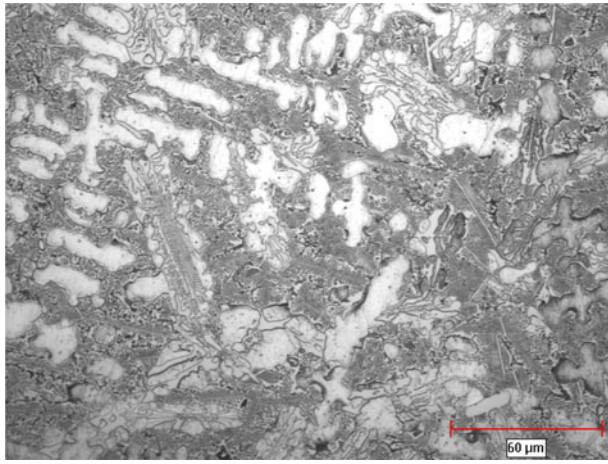


Fig. 7—SEM micrograph of a brazement produced by using 100 pct BPPs.

APPs during equilibration, the lower the extent of solutal melting of APPs. According to Fick's second law of diffusion, the kinetics of solute-transport by solid-state diffusion is controlled by the extent of change in solute concentration gradient per unit distance  $\left[\frac{\partial}{\partial x} \left(\frac{\partial C}{\partial x}\right)\right]$  away from the liquid–solid interface within the APPs. A major factor that influences  $\frac{\partial}{\partial x} \left(\frac{\partial C}{\partial x}\right)$  is the particle size—at any given time subsequent to the initial diffusion of the MPD solute into the APPs during the equilibration process, the smaller the initial particle size, the lower the  $\frac{\partial}{\partial x} \left(\frac{\partial C}{\partial x}\right)$  and the slower the solute-loss kinetics and the higher the extent of APPs melting. Accordingly, complete melting of the fine APPs is attributable to insufficient solute-loss to complement partial solutal melting of the APPs to achieve equilibration of the liquid, because of inhibited solid-state diffusion caused by low  $\frac{\partial}{\partial x} \left(\frac{\partial C}{\partial x}\right)$ . This is in contrast to the case of coarse APPs, where the extent of solute-loss seems sufficient to complement partial solutal melting to achieve equilibration of the liquid, because of a larger  $\frac{\partial}{\partial x} \left(\frac{\partial C}{\partial x}\right)$ .

Micro-hardness testing showed that the eutectic products in the brazements exhibit about 250 pct higher hardness compared to the residual APPs, 407 HV for the eutectic vs 148 HV for the APPs. It has been found that hard and brittle eutectic products constitute a major cause of degradation of mechanical properties, including fatigue behavior, in brazed materials, by promoting crack initiation and propagation.<sup>[7,8]</sup> In the current study, the effects of complete and partial meltings of fine and coarse APPs, respectively, on fatigue life of brazed specimens were investigated to confirm the reported damaging influence of the hard eutectic microconstituents. The results of the fatigue tests, Figure 8, show that the fatigue life reduced by about 66 pct by using fine APPs compared with the coarse APPs. Notwithstanding the incorporation of 50 pct fine APPs in the interlayer mixture, which normally would have been expected to translate to a better mechanical performance, the fine APPs brazement exhibited a degraded fatigue life that is compara-

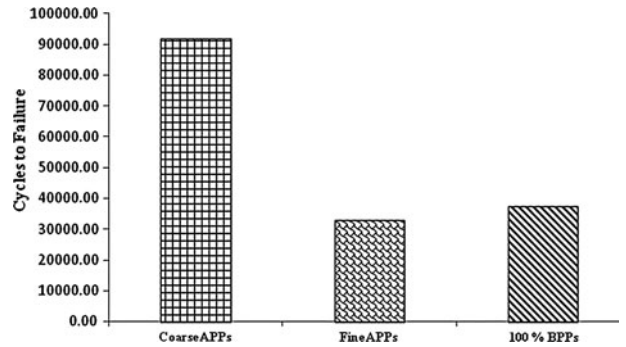
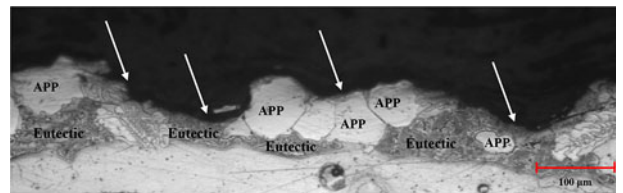
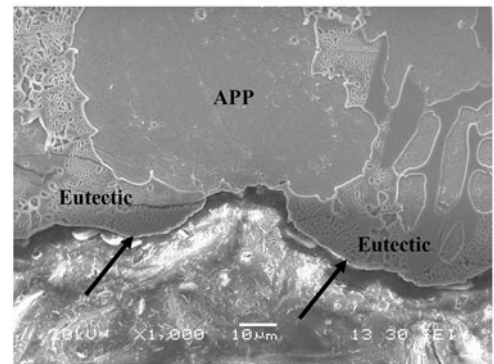


Fig. 8—Fatigue lives of 50 pct coarse and 50 pct fine APPs and 100 pct BPPs brazements.



(a)



(b)

Fig. 9—(a) Arrows show a fatigue crack path that preferentially propagated through eutectic microconstituents; (b) SEM higher magnification micrograph of the crack path, which is shown by arrows.

ble with the brazement produced by using 100 pct BPPs free of APPs (Figure 8). This is because both the fine APPs and 100 pct brazing alloy brazements have a similar microstructure that entirely consists of deleterious eutectic microconstituents, caused by complete melting of all the BPPs and APPs. Microstructural study of fatigue-fractured specimens showed that fatigue cracks preferentially propagated along the eutectic products and, in contrast, by-passed the residual APPs in coarse APPs brazement (Figure 9). Therefore, even though solute-loss is generally neglected during analytic modeling of wide-gap brazing, the current experimental research, which not only confirms our previous numerical simulation result but also shows that fatigue life of brazed materials is significantly influenced by the solute-loss effect. In order to improve the fatigue life of wide-gap brazement, this research shows that adequate solute-loss into APPs during equilibration, which is

necessary to prevent complete solutal melting of the APPs, but is not generally considered, is crucial.

---

The authors would like to thank NSERC of Canada for financial support.

### REFERENCES

1. O.A. Ojo, N.L. Richards, and M.C. Chaturvedi: *Metall. Mater. Trans. A*, 2006, vol. 37A, pp. 421–33.
2. B. Radhakrishnan and R.G. Thomson: *Metall. Trans. A*, 1993, vol. 24A, pp. 1409–22.
3. R. Thamburaj, W. Wallace, and J.A. Goldak: *Int. Met. Rev.*, 1983, vol. 28, pp. 1–22.
4. W. Chen, M.C. Chaturvedi, and N.L. Richards: *Metall. Mater. Trans. A*, 2001, vol. 32A, p. 931.
5. M.B. Henderson, D. Arrell, M. Larsson, and G. Marchant: *Sci. Technol. Weld. Join.*, 2004, vol. 9, p. 13.
6. G. Cam and M. Kocak: *Int. Mater. Rev.*, 1998, vol. 43, p. 1.
7. X. Huang and W. Miglietti: *J. Eng. Gas Turbines Power*, 2012, vol. 134, pp. 1–17.
8. X.W. Wu, R.S. Chandel, H.P. Seow, and H. Li: *J. Mater. Process. Technol.*, 2001, vol. 113, pp. 215–21.
9. Y.H. Yu and M.O. Lai: *J. Mater. Sci.*, 1995, vol. 30, pp. 2101–07.
10. J.H.G. Mattheij: *Mater. Sci. Technol.*, 1985, vol. 1, pp. 608–12.
11. L.C. Lim, W.Y. Lee, and M.O. Lai: *Mater. Sci. Technol.*, 1995, vol. 11, pp. 955–60.
12. Y. Zhou, W.F. Gale, and T.H. North: *Int. Mater. Rev.*, 1995, vol. 40, pp. 181–96.
13. A. Ghoneim, J. Hunedy, and O.A. Ojo: *Metall. Mater. Trans. A*, 2013, vol. 44A, pp. 1139–51. DOI:10.1007/s11661-012-1412-1.
14. P. Villars, A. Prince, and H. Okamoto: *Handbook of Ternary Alloy Phase Diagrams*, ASM International, Metals Park, OH, 1993.
15. K. Ohsassa, T. Shinimura, and T. Narita: *J. Phase Equilib.*, 1999, vol. 20, p. 199.